Supporting Information

A role for the fifth G-track in G-quadruplex forming oncogene promoter sequences during oxidative stress: Do these "spare tires" have an evolved function?

Aaron M. Fleming,[1†] Jia Zhou,[2†] Susan S. Wallace,[2*] and Cynthia J. Burrows[1*]

[1]Department of Chemistry, University of Utah, Salt Lake City, UT 84112, USA and

[2]Department of Microbiology and Molecular Genetics, University of Vermont, Burlington, VT 05045, USA

*To whom correspondence should be addressed.

E-mail: burrows@chem.utah.edu or susan.wallace@uvm.edu

[†]These authors contributed equally to the conception of this manuscript.

Detailed Experimental Methods

Oligomer preparation. All oligomers were synthesized by the DNA Peptide core facility at the University of Utah following standard protocols. The site specific introduction of the OG was achieved via the OG phosphoramidite (Glen Research, Sterling, VA) following the manufacturer's protocols for the cleavage and deprotection. The crude oligomers were purified using ion-exchange HPLC using a semi-preparative column running the following mobile phases: A = 1.5 M LiOAc (pH 7) in 1:9 MeCN:ddH_2O; B = 1:9 MeCN:ddH_2O. The method was initiated at 5% B followed by a linear gradient to 100% B over 30 min with a flow rate of 3 mL/min while monitoring the absorbance at 260 nm. The purified samples were dialyzed against ddH_2O for 36 h to remove the purification salts, followed by lyophilization to concentrate the samples. The dried samples were resuspended in ddH_2O, and the concentrations were determined by the absorbance at 260 nm, using the nearest neighbor approximation to determine the extinction coefficient. Substitution of G for OG and omitting a nucleotide for Gh was used to estimate the extinction coefficients for these strands. (The absorbance profile for Gh is nearly 0 at 260 nm.[1]) The purified stands were annealed at the desired concentration by heating them to 90 °C for 5 min followed by slowly cooling to room temperature of ~3 h, and then placing the samples at 4 °C for 48 h prior to analysis.

Synthesis of the Gh-containing strands was achieved following previously described methods that are elaborated in Figure S3. The Gh strands were purified on an analytical ion-exchange HPLC column running the same mobile phases and monitoring conditions as described above, with the exception that the flow rate was 1 mL/min. The purified Gh samples were dialyzed against ddH_2O for 36 h and concentrated by lyophilization.

The ESI-MS oligomer samples were prepared by repurification of the sample using a reversed-phase HPLC column running A = 20 mM NH_4OAc (pH 7) and B = MeCN to replace the residual monovalent cations with ammonium ions that are MS compatible. The purified samples were dried and dialyzed against 3 mM NH_4OAc for 24 prior to MS analysis. The analysis was conducted by the Mass Spectrometry facility in the Dept. of Chemistry at the University of Utah.

Oxidation Reaction Conditions: 10 μM *VEGF*-4 at 37 °C 20 mM cacodylic acid (pH 7.4) + 140 mM KCl +12 mM NaCl + 200 mM $KHCO_3$ + 20 mM $K_2S_2O_8$ and 254 nm light for 20 min to produce $CO_3^{\bullet-}$ when NAC was present; 3 mM SIN-1 and 25 mM $KHCO_3$ for reactions without NAC; or, 50 μM riboflavin + 350 nm light for 10 min. Sites of reaction were determined by hot piperidine cleavage for 2 h, which revealed <20% reactivity. These piperidine conditions should uncover ~75% of the Sp reaction sites, ~100% of the Gh sites, and the OG sites were determined by further oxidation with Na_2IrCl_6 before piperidine treatment.[2]

Thermal melting analysis. The UV melting studies were conducted on a Shimadzu UV-vis spectrometer running their software. The T_m values were determined on samples of 1 μM quadruplex in buffered solutions with physiological salt concentrations (20 mM cacodylate pH 7.4, 140 mM KCl, and 12 mM NaCl). The melting experiments were initiated by thermally equilibrating the samples at 20 °C for 10 min followed by heating the samples at 0.5 °C/min and equilibrating at each 1 °C increment for 1 min. A reading at 260 and 295 nm was taken after each 1 °C change in the temperature. The heating phase involved increasing the temperature

to 95 °C followed by a 10 min hold and then a return to 20 °C via the same change in temperature and increment time while making absorbance readings at each 1 °C change. Plots of absorbance at 295 nm vs. temperature were constructed, and the T_m value was determined from the first derivative of the curve, as well as by a two-point analysis protocol using the instrument's software. The T_m studies to determine the number of coordinated K^+ ions (ΔnK^+) was conducted using the same quadruplex concentrations but the salt conditions were changed to 20 mM cacodylate (pH 7.4) with 20, 50, 70, 100, 150, and 200 mM KCl. Plots of T_m vs. ln[KCl] were constructed for data analysis by literature methods[3] that is more thoroughly described in Figure S5.

CD Spectroscopy. The CD spectra were recorded on 10 μM quadruplex samples in 20 mM cacodylate (pH 7.4) with 140 mM KCl and 12 mM NaCl at 20 °C. The CD readings in mdeg were converted to molar ellipticities for presentation purposes.

DMS Footprinting Assays. First, the quadruplex samples were 5`-labeled with ^{32}P via standard protocols.[4] To a 10 μM solution of quadruplex that was not labeled with ^{32}P, was added 20,000 cpm of ^{32}P-labeled quadruplex. The mixture was annealed in buffer with physiological salt concentrations (20 mM cacodylate (pH 7.4), 140 mM KCl, and 12 mM NaCl) via the method outlined above. To the samples was added 0.1 μg/μL of calf thymus DNA, and then the samples were thermally equilibrated at 37 °C prior to dimethyl sulfate (DMS) addition. Next, DMS was added to a final concentration of 1% (v/v) and the samples were incubated for either 0.5 or 1 min, and then they were quenched with 0.5 M β-mercaptoethanol. The quenched samples were dialyzed against ddH_2O overnight followed by lyophilization to dryness. The dried samples were resuspended in 100 μL of freshly prepared, aqueous 1 M piperidine solution and then incubated at 90 °C for 30 min. After hot piperidine treatment the samples were lyophilized to remove the piperidine and then resuspended in gel loading dye (0.25% each of bromophenol blue and xylene cyanol in 30% (v/v) aqueous glycerol). The samples were loaded onto a 20% PAGE and electrophoresed at 75 W for 4 h. The electrophoresed gel was then loaded into a phosphor screen and left to expose for 18 h, followed by imaging via phosphorimager autoradiography. The bands were visualized using ImageQuant software.

Enzyme purification

Glycosylases used in this study were from lab stocks. Cloning, expression, and purification of the glycosylases OGG1,[5] NTH1,[6] NEIL1,[6] NEIL2,[5] and the glycosylase domain of NEIL3 (NEIL3-GD)[7] were previously described. The percentage of active glycosylase was determined by the Schiff base assay,[5] and all protein concentrations reported in this study were corrected for the active enzyme percentage.

DNA substrate preparation

Lesion-containing ODNs were ^{32}P-labeled at the 5' end by T4-polynucleotide kinase (NEB). The labeled ODNs were ethanol precipitated as previous described.[8] Substrates contain 1 part hot ODN and 9 parts cold ODN. All G4-forming ODNs were annealed in quadruplex folding buffer (Qu buffer), which contains 20 mM HEPES-KOH (pH 7.4), 100 mM KCl and 1 mM EDTA. To fold quadruplex DNA, the ODN in Qu buffer (ODN concentration = 100 nM) was heated at 90 °C

for 3 min and slowly cooled to room temperature. The mixture was then stored at 4 °C overnight before conducting the assays. To make duplex DNA, a 1.2-fold excess of the complementary strand to the lesion-containing strand were annealed at 90 °C for 3 min and then slowly cooled to room temperature.

Glycosylase activity assays

Glycosylase assays were done in the quadruplex reaction buffer, which contains 20 mM HEPES-KOH pH 7.4, 100 mM KCl, 1 mM EDTA, 0.1 mg/ml BSA and 1 mM DTT. Substrate concentrations were typically 10 nM, unless otherwise specified and enzyme concentrations are indicated in the figure legends. Enzymes and substrates were incubated at 37 °C. To measure only the glycosylase activity, reactions were terminated by adding NaOH to a final concentration of 0.2 N and heated at 95 °C for 5 minutes. An equal volume of FE buffer (96% formamide, 20 mM EDTA, 0.1% bromophenol blue, and 0.1% xylene cyanol) was added to the reactions before loading on a 16% urea gel for separation. The gel was dried and exposed on a phosphorimager screen. Finally, bands from the screen were scanned by Molecular Imager PharosFX Plus (Bio-Rad Laboratories) and quantified by Quantity One software (Bio-Rad Laboratories).

Table S1. List of other proposed regulatory promoter G4s with the "spare tire" domain and other G4s with the same feature. Some of these sequences have more than one additional G-track. Acceptable 5th domains were identified within 13 nucleotides of the core G4 sequence, on the basis of recent reports.[9]

Name	Sequence
VEGF [10]	5`-GGGG C GGG CC GGGGG C GGGG TCCCGGC GGGG
c-MYC [11]	5`-GGGG A GGG T GGGG A GGG T GGGG
HIF-1α [12]	5`-GGG CGCGC GGGG A GGGG AGA GGGGG C GGG
BCL-2 [13]	5`-GGGG C GGG CGC GGG AGGAA GGGGG C GGG
RET [14]	5`-GGG TA GGGG C GGGG C GGGG C GGGGG
KRAS [15]	5`-GGG AGCGGCTGA GGG CGGTGT GGG AAGA GGG AAGA GGGGG
HSP90 [16]	5`-GGG C GGG CCAAA GGG AA GGGG T GGG
PDGFR-β [17]	5`-GGG AGAA GGGGGGG CGGC GGGG CA GGG A GGG
AR [18]	5`-GGGG A GGGG AGA_4GGA_3 GGGG A GGGG A GGG
ADAM[19]	5`-GGGG CC GGG T GGG A GGGGG C GGG CC GGGG C GGGG
SRC[20]	5`-GGG TCCCCT GGG CCT GGG C GGG AGC GGGG A GGGG
b-RAF[21]	5`-GGG C GGGG A GGGGG AA GGG AGGCGGAGAGCT GGGGG
b-RAF[21]	5`-GGGGGG CGC GGGGGG CGC GGGG AGGAGCGGCCC GGG
YinYang[22]	5`-GGGG A GGG A GGGG CCGGCC GGG AGC GGGG TTGAGGC GGG T GGG
hTERT[23]	5`-GGGG A GGGG CT GGG A GGG CCCGGA GGGGG CT GGG CC GGGG ACCC GGG A GGGG TC GGG AC GGGG C GGGG
c-MYB[24]	5`-GGA GGA GGA GGTCAC GGA GGA GGA GGA GAA GGA GGA GGA GGA
MET[25]	5`-GGG AGTGCGGCCGGC GGG C GGG C GGG GCGCT GGG
PKD2[26]	5`-GGG TGGAA GGG CTC GGG C GGGG A GGG
Nrf2[27]	5`-GGG AA GGG AGCAA GGG C GGG A GGG
Repeat sequences	
hTelo[12]	5`-GGG TTA GGG TTA GGG TTA GGG TTA GGG
C9orf72[28]	5`-GGGG CC GGGG CC GGGG CC GGGG CC GGGG
GGC Repeat[12]	5`-GG C GG C GG C GG C GG

Figure S1. G-oxidation sites and products in *VEGF*-4 folded as a G4 or as a duplex.

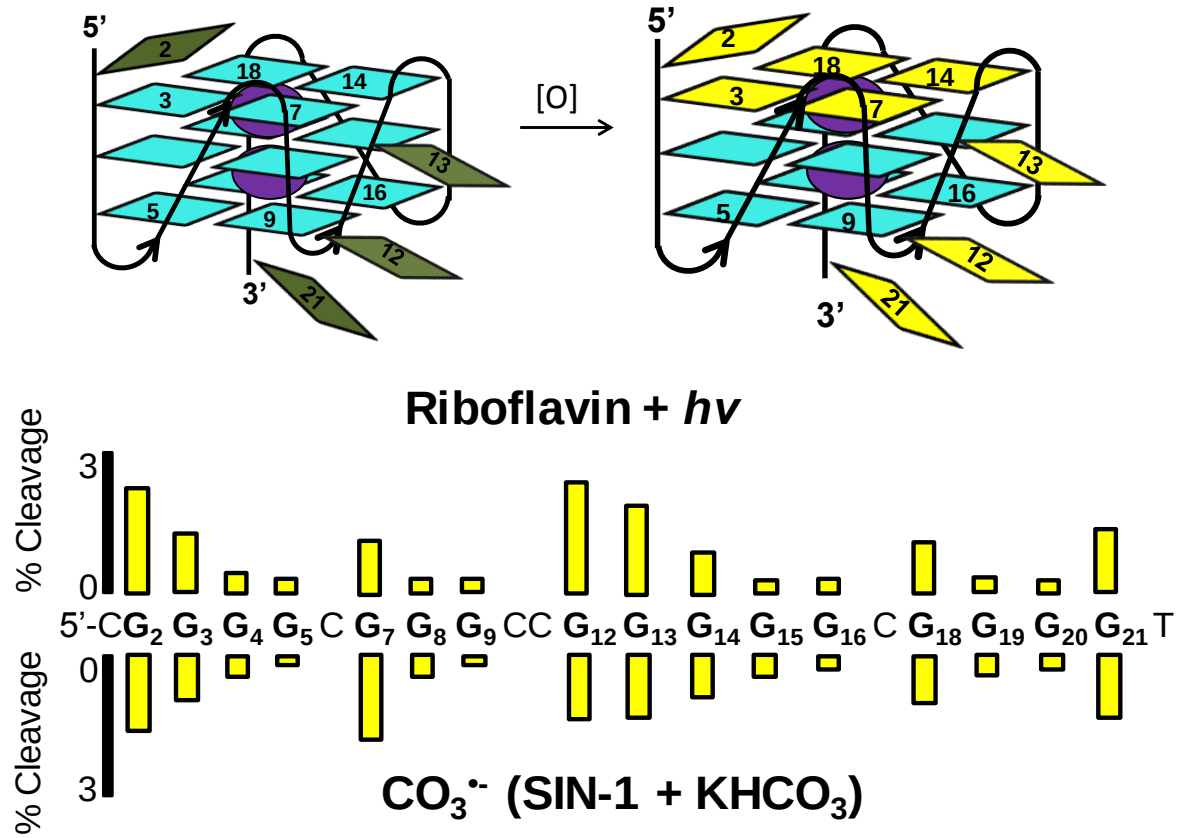

Observations: The most reactive G sites toward oxidation are found in the loops or are the 5`-G in the core. Loop Gs are ~1.5-2x more reactive than core Gs.

Figure S1. Cont.

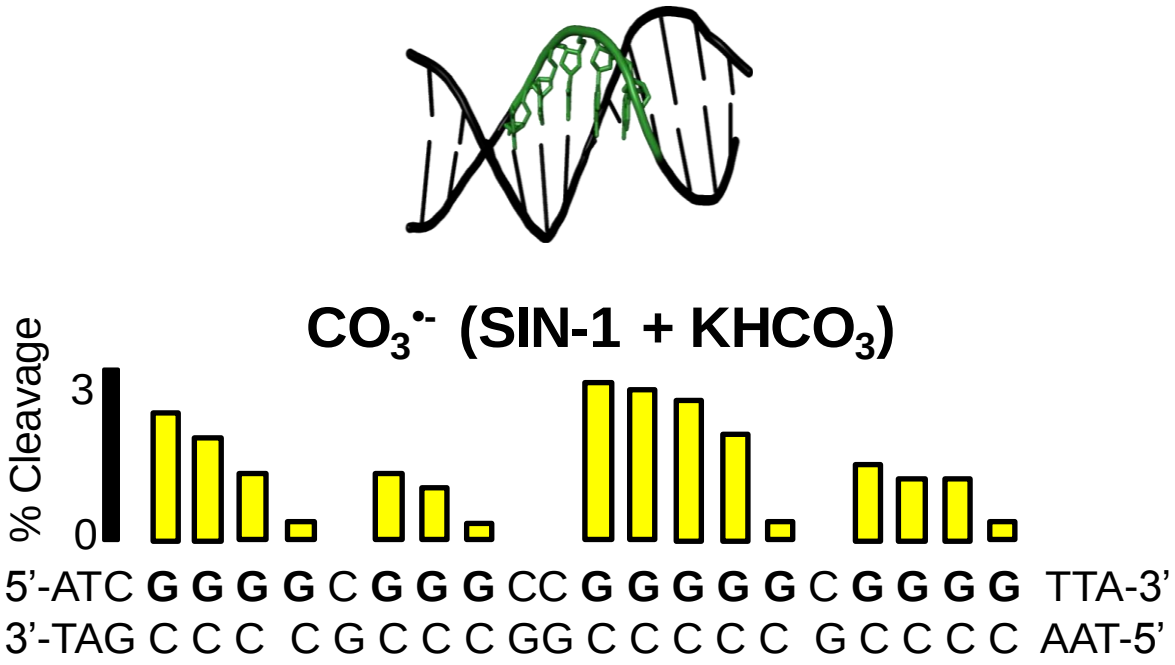

Observations: In the duplex context, reactivity toward oxidation was enhanced at the Gs located 5' to another G.

Figure S2. Products detected upon oxidation of *VEGF*-4 in the G4 and duplex contexts.

Products characterized when the *VEGF*-4 G4 fold or duplex were oxidized with one-electron oxidants

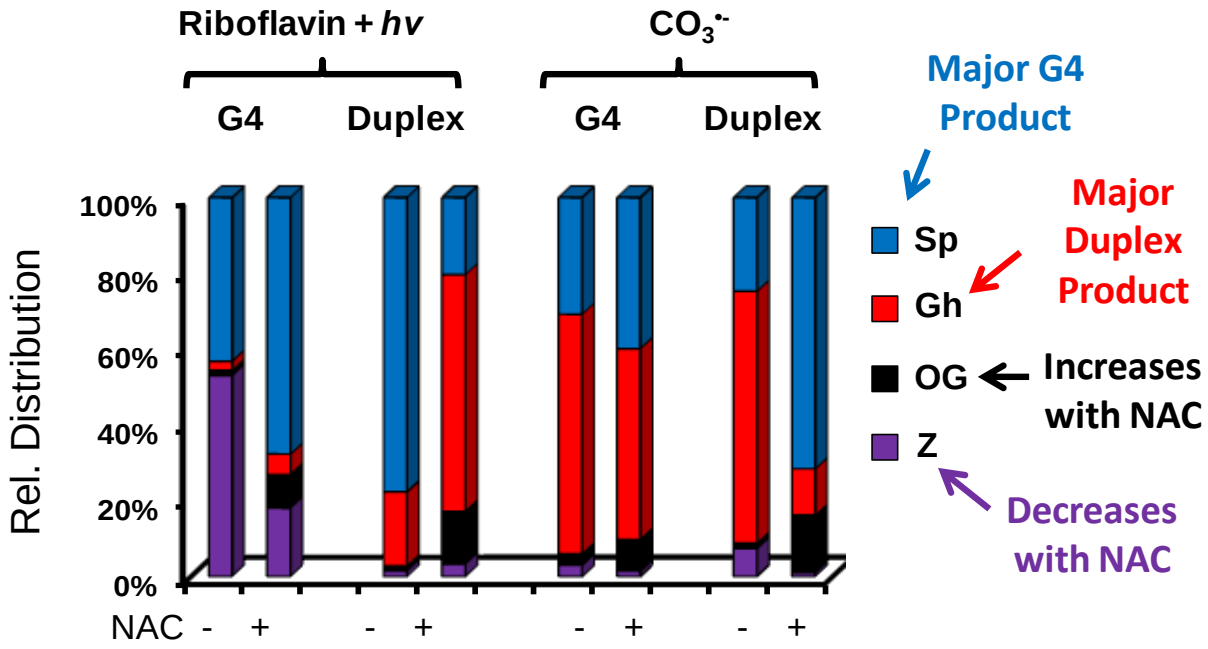

VEGF-4 = 5`-C GGGG C GGG CC GGGGG C GGGG T-3`

Product analysis was determined by nuclease digestion and LC-MS analysis after low conversion oxidation (<12% conversion) via literature methods.[29] Because of the G-rich nature of these strands, control of the reactivity was very challenging. Key observations include Gh as a major product in the duplex context, and Sp as a major product in the G4 context, and low levels of OG, the intermediate to Sp and Gh,[1,30] were observed in all oxidations. The yield of oxazolone (Z) was greatest with oxidations catalyzed with photoexcited riboflavin because of the release of superoxide, a reaction partner with oxidized G leading to Z. This product dramatically diminishes when relevant amounts of reductant, such as *N*-acetylcysteine, are added to the reaction mixture that quenches the intermediate superoxide.[31]

Figure S3. Synthesis and characterization of the oligomers studied.

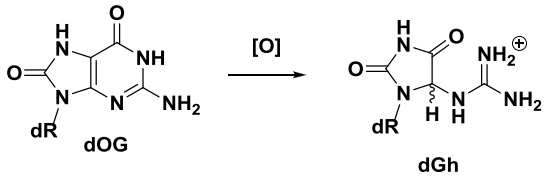

Ion-exchange HPLC to demonstrate oligomer purity

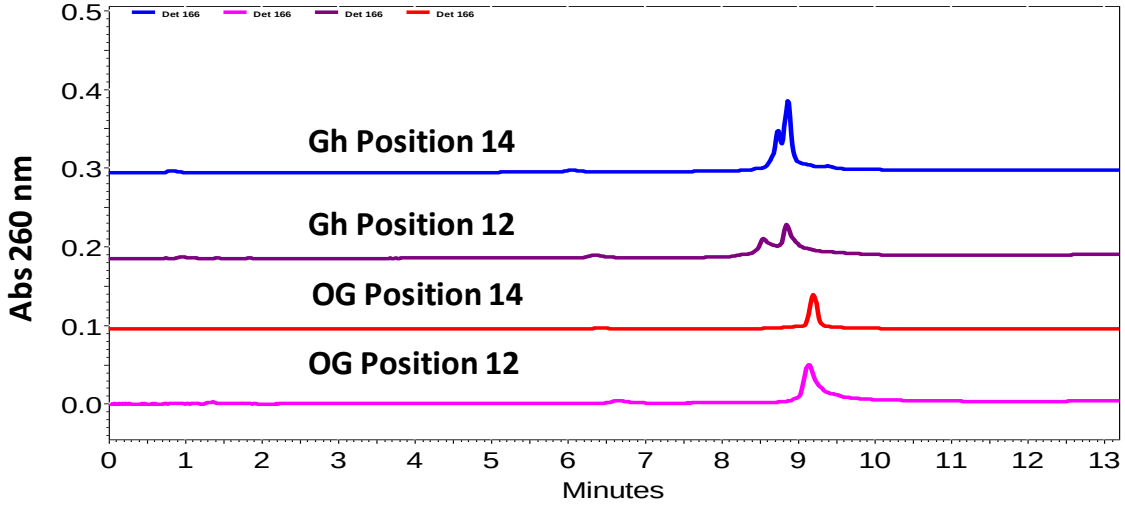

5'-CG GGG C GGG CC**G**$_{12}$G **G**$_{14}$GG C GGG GT

Synthesis- 10 µM DNA, 120 µM K_2IrBr_6, in ddH_2O at 20 ^oC with 50 mM 18c6
Purification- Ion-exchange HPLC with A = 1 M LiCl, 25 mM Tris (pH 8) and 10% MeCN; B = 10% MeCN and 90% ddH_2O. The two peaks observed for Gh represent the two diastereomers of this product; also, these diastereomers readily interconvert rendering their individual study nearly impossible.[32]

Mass Spectrometry Data for *VEGF*-4 Sequences

Sequence	Calcd Mass	Exp Mass
VEGF	**6954.5**	**6954.8**
***VEGF* OG pos 12**	**6970.5**	**6971.4**
***VEGF* Gh pos 12**	**6960.5**	**6960.5**
***VEGF* OG pos 14**	**6970.5**	**6971.2**
***VEGF* Gh pos 14**	**6960.5**	**6960.8**
***VEGF* OG pos 7**	**6970.5**	**6971.5**
***VEGF* Gh pos 7**	**6960.5**	**6960.1**

Figure S3. Continued

VEGF-5 HPLC Traces

Ion-exchange HPLC Chromatogram

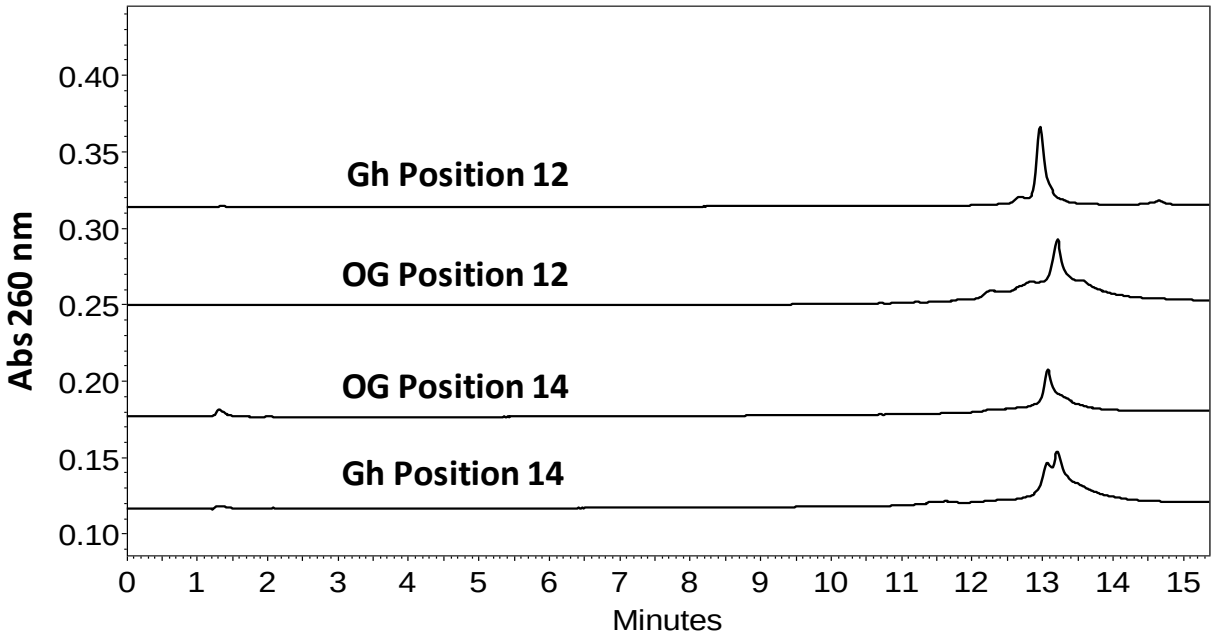

Mass Spectrometry Data for the *VEGF*-5 Sequences

Sequence	Calcd Mass	Exp Mass
***VEGF*-5**	**10,375.7**	**10,376.1**
***VEGF*-5 OG pos 12**	**10,391.7**	**10,392.7**
***VEGF*-5 Gh pos 12**	**10,381.7**	**10,381.9**
***VEGF*-5 OG pos 14**	**10,391.7**	**10,392.3**
***VEGF*-5 Gh pos 14**	**10,381.7**	**10,381.4**

Exp masses were obtained by ESI^--MS
Acceptable error ~ 0.02% (~ 1 mass unit).

Figure S4. Reversibility of the thermal melting process and van 't Hoff analysis of the T_m data.

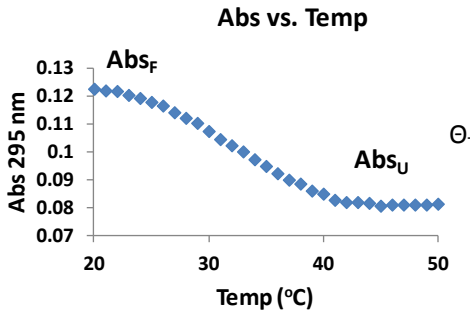

$$\Theta_T = \frac{(Abs_T - Abs_U)}{(Abs_F - Abs_U)}$$

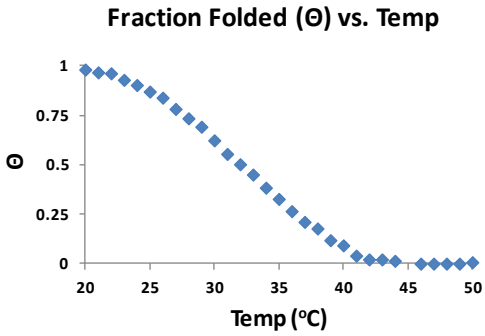

$$K_a = \Theta_T/(1- \Theta_T)$$

Calculation of Thermodynamic Values

$y = mx + b$

$m = -\Delta H/R \quad b = \Delta S/R$

$R = 1.987$ cal/mol K

$\Delta G = \Delta H - T\Delta S$

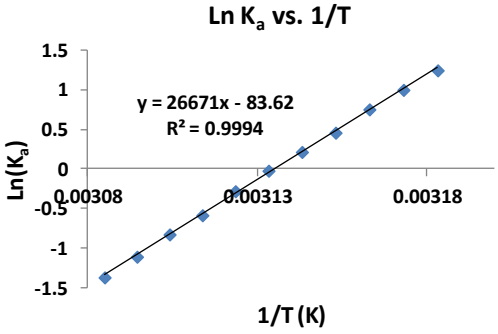

Mergny, J-L.; Lacroix, L. *Curr. Protocols in Nucleic Acids Chem.* **2009**, 17.1.1 - 17.1.15.

VEGF Sequence	T_m (°C)	ΔG_{vH} 37 °C (kcal/mol)	ΔH_{vH} (kcal/mol)	ΔS_{vH} (cal/mol*K)	ΔnK^+
WT	**85.6 ± 0.8**	**-8.9 ± 1.2**	**-75.9 ± 9.9**	**-216 ± 33**	**2.3**
OG 12 Loop	83.2 ± 0.7	-8.5 ± 1.0	-74.8 ± 9.1	-214 ± 26	**2.4**
Gh 12 Loop	85.5 ± 0.7	-8.2 ± 1.0	-70.2 ± 8.4	-200 ± 25	**2.1**
OG 14 Core	**58.6 ± 0.8**	**-2.8 ± 0.4**	**-33.5 ± 3.7**	**-99 ± 12**	**1.2**
Gh 14 Core	**63.4 ± 0.6**	**-4.4 ± 0.5**	**-41.3 ± 4.9**	**-119 ± 14**	**1.5**
OG 7 Loop	**56.3 ± 0.7**	**-3.2 ± 0.4**	**-42.7 ± 5.1**	**-127 ± 15**	**1.3**
Gh 7 Loop	**58.1 ± 0.8**	**-3.6 ± 0.4**	**-39.8 ± 4.8**	**-116 ± 14**	**1.6**

The thermodynamic constants reported were determined at pH 7.4 with 150 mM K^+ ion present.

Figure S5. KCl-concentration dependent T_m studies with *VEGF*-4 and *VEGF*-5 with and without damage at the loop and core positions studied.

Example set of T_m curves

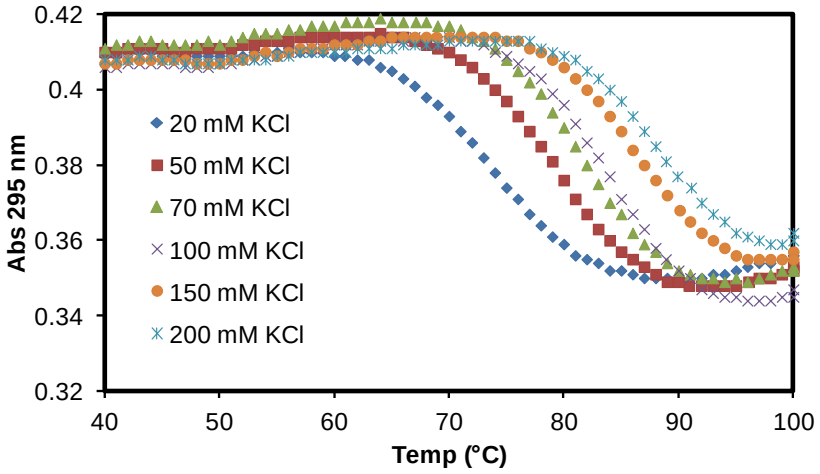

Plots of T_m vs. [KCl] for the *VEGF*-4 sequences

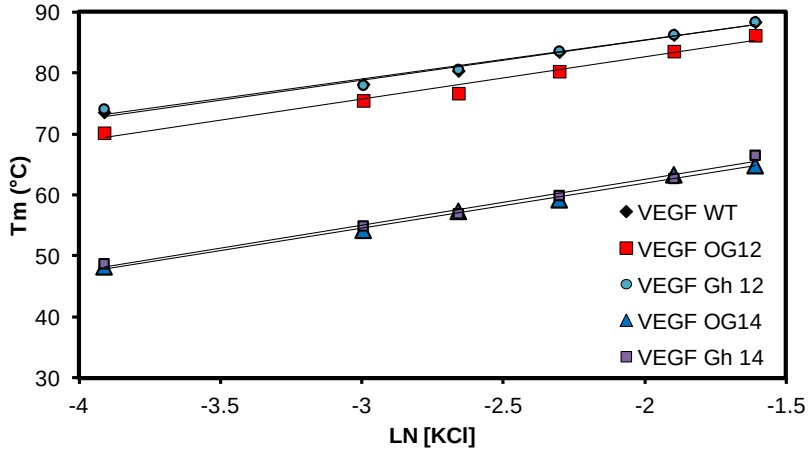

Estimation of the number of bound K^+ ions by the G4 fold (ΔnK^+) was achieved using the equations described in the literature.[3] Briefly, van 't Hoff analysis allowed measurement of the ΔH for each sequence that was used in the following equation for to determine ΔnK^+, where $\Delta nK^+ = 1.11 * \Delta H/(R*T_m^2) *$ slope. Cautionary point: We are aware that using T_m curves to estimate thermodynamic properties is not the best approach; however, the better approach, differential scanning calorimetry, requires far more sample than can reasonably be synthesized for these damage-containing strands. For ΔnK^+ values determined see the table on the previous page. All T_m values have errors of approximately ±0.8 °C.

Figure S5. Continued

VEGF Sequence	T_m (°C)	ΔG_{vH} 37 °C (kcal/mol)	ΔH_{vH} (kcal/mol)	ΔS_{vH} (cal/mol*K)	ΔnK^+
WT	79.1 ± 0.6	-5.4 ± 0.6	-57.8 ± 6.4	-169 ± 19	**2.1**
OG 7 Core	78.6 ± 0.9	-6.0 ± 0.8	-59.0 ± 6.6	-171 ± 18	**2.6**
Gh 7 Core	79.8 ± 0.8	-6.4 ± 0.8	-61.2 ± 7.3	-176 ± 20	**2.5**
OG 12 Loop	80.1 ± 0.7	-7.4 ± 0.8	-63.8 ± 7.3	-182 ± 21	**2.4**
Gh12 Loop	80.5 ± 0.9	-6.5 ± 0.8	-59.7 ± 7.1	-172 ± 20	**2.3**
OG 14 Core	81.1 ± 0.8	-8.5 ± 1.0	-62.4 ± 7.5	-174 ± 20	**2.3**
Gh14 Loop	83.0 ± 0.7	-7.8 ± 0.8	-61.9 ± 7.3	-175 ± 23	**2.2**

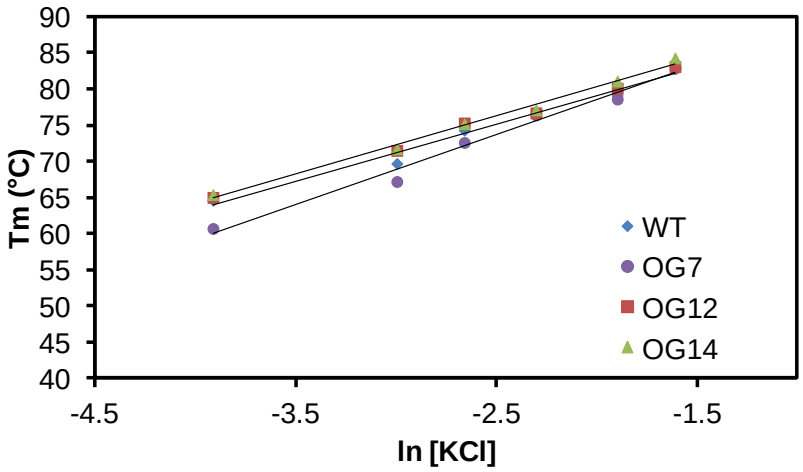

Figure S6. CD spectra for Gh-containing *VEGF*-4 and *VEGF*-5 sequences.

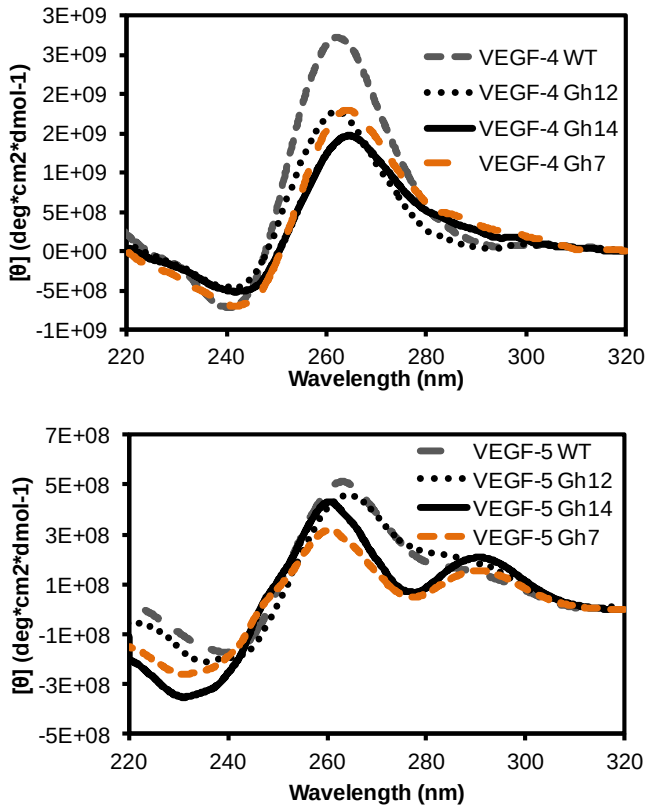

The CD spectra were determined in buffered physiological salt conditions (20 mM cacodylate pH 7.4, 140 mM KCl, and 12 mM NaCl) at 20 °C.

Figure S7. DMS footprinting results for the VEGF-5 sequences.

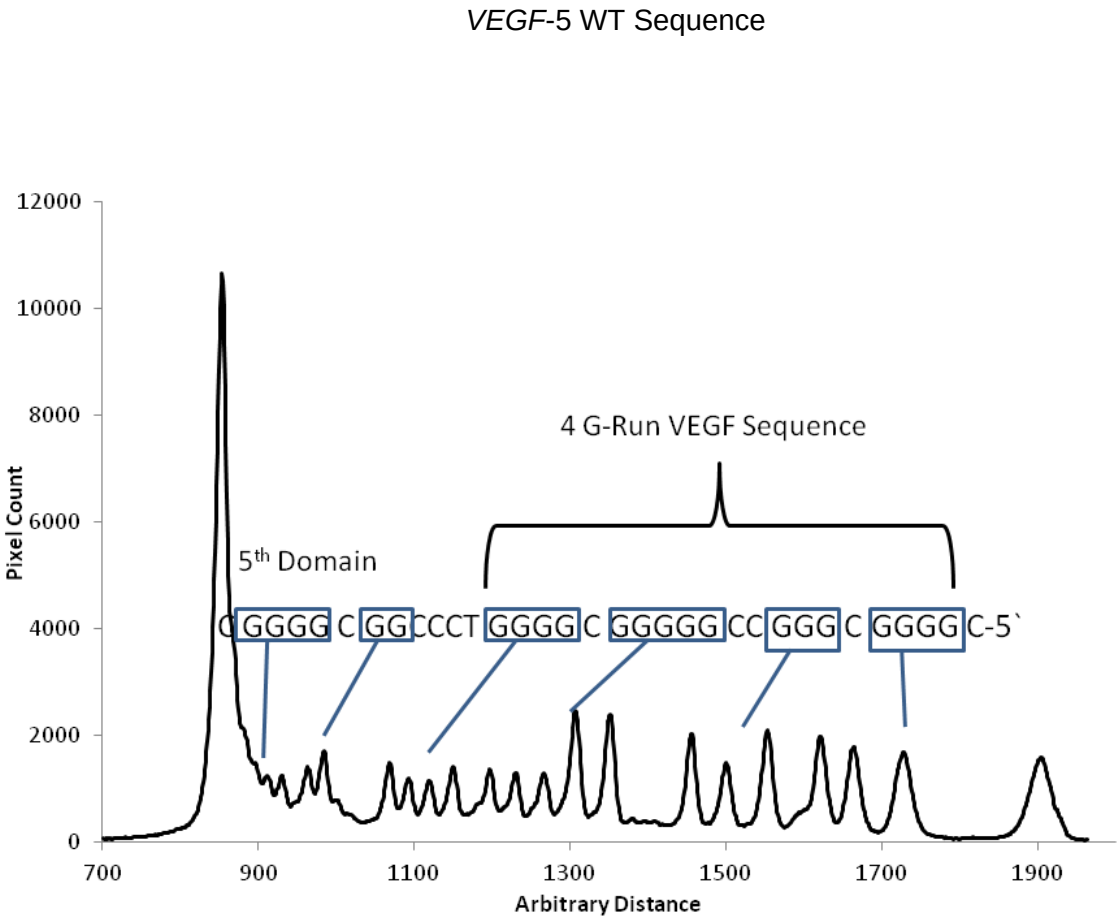

140 mM KCl + 12 mM NaCl pH 7.4 at 20 °C with 1% DMS for 1 min

Figure S7. Continued

VEGF-5 OG12

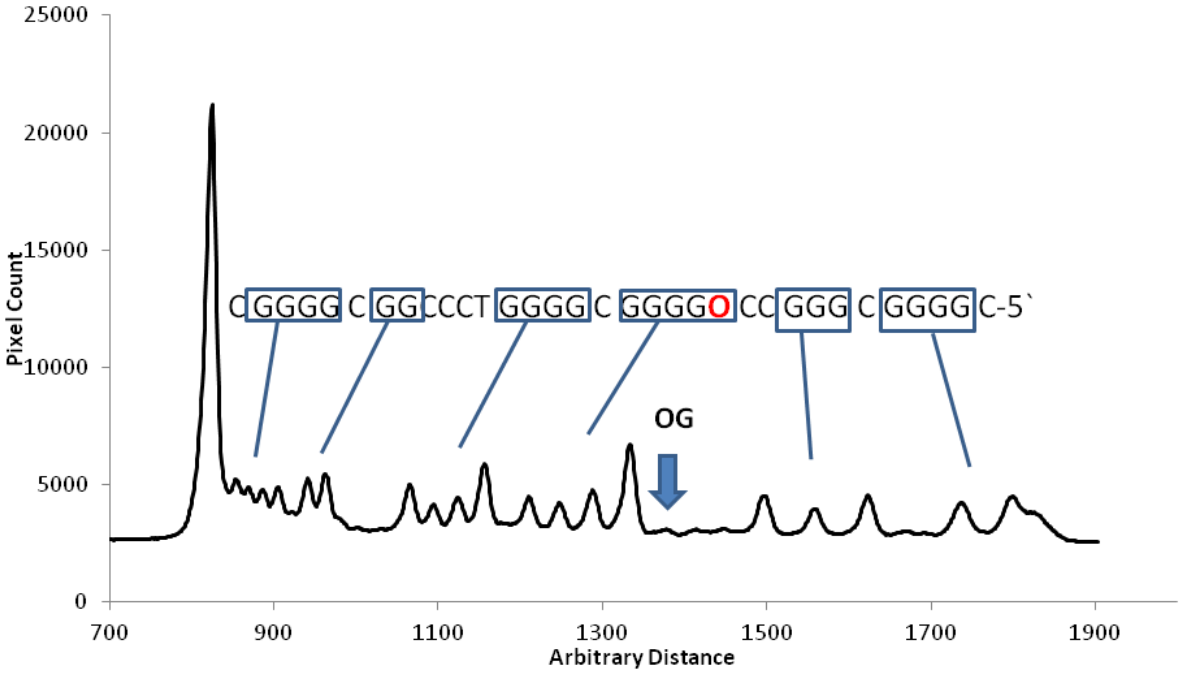

Figure S7. Continued

VEGF-5 OG14

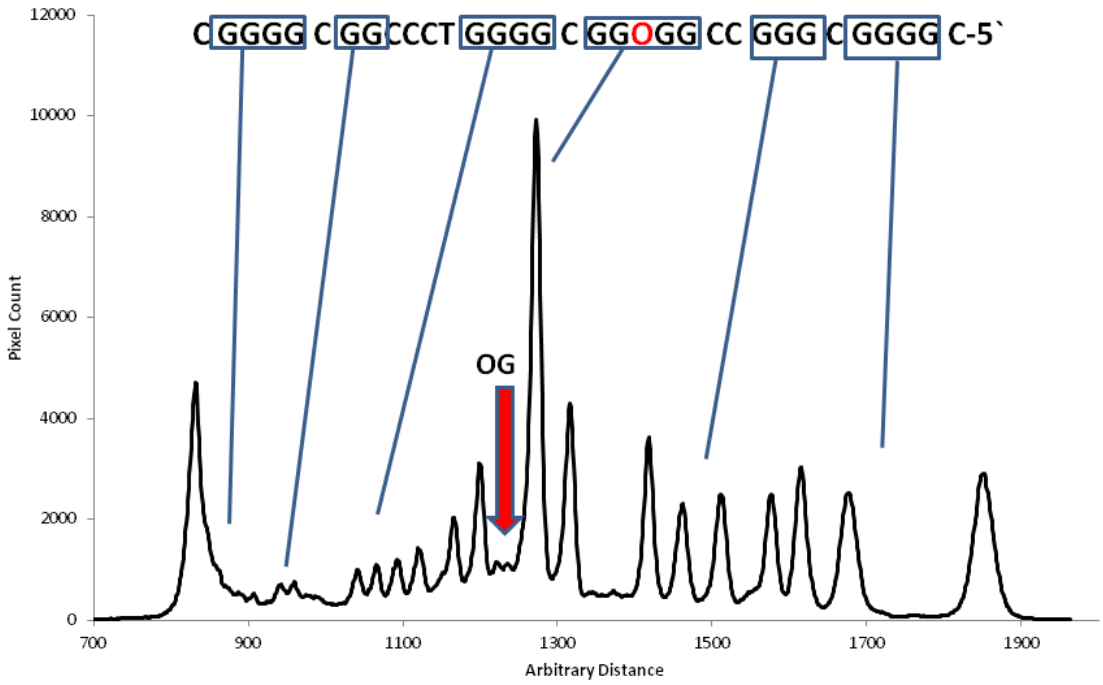

DMS footprinting assays were not conducted with Gh-containing *VEGF*-5 strands because Gh is very piperidine labile.[2]

Figure S8. A representative gel from the NEIL1 time-course assay conducted on the Gh-containing *VEGF*-5 sequence. Reaction conditions included 10 nM of each substrate incubated with 10 nM of glycosylase at 37 °C for 20 min, and the reactions were quenched by adding NaOH and heating at 95 °C for 5 min.

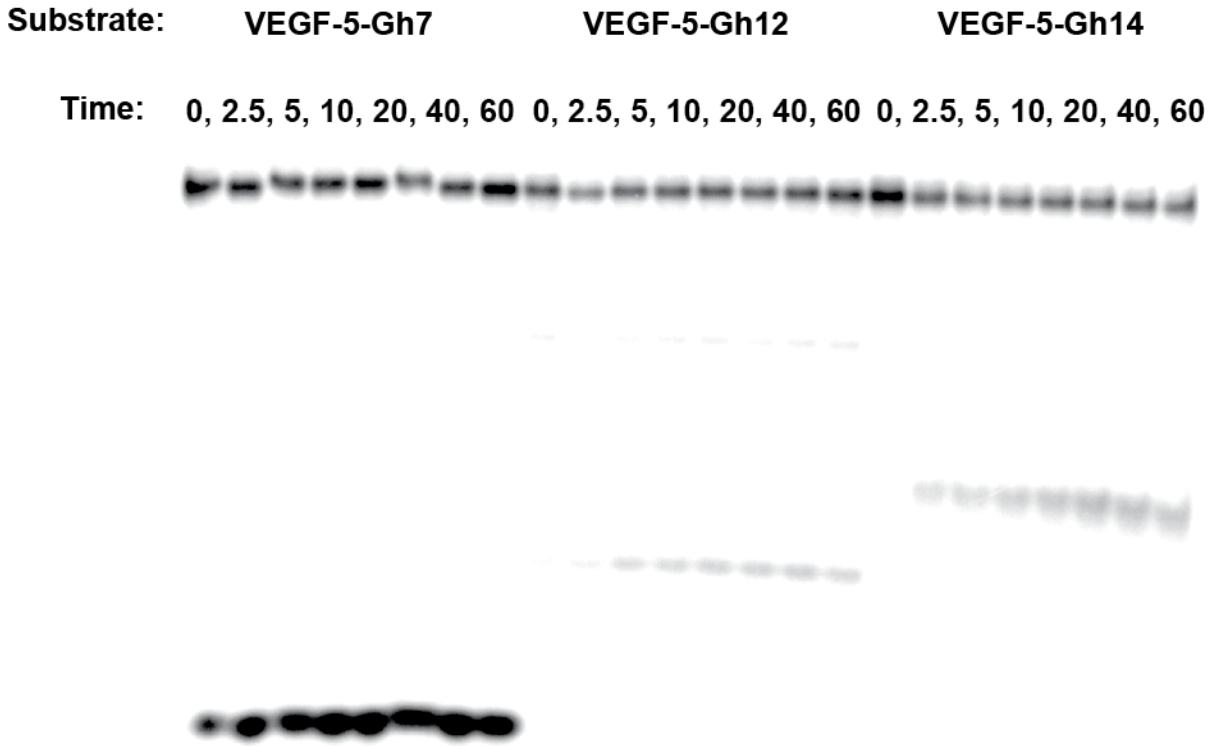

Figure S9. A representative gel from the glycosylase assay conducted on OG-containing *VEGF*-5. Reaction conditions included 10 nM of each substrate incubated with 10 nM OGG1 at 37 °C for 20 min, and the reaction was stopped by adding NaOH and heating. Quantification of OG removal by OGG1 was detemrined. Mean and standard deviation from four replicates are shown.

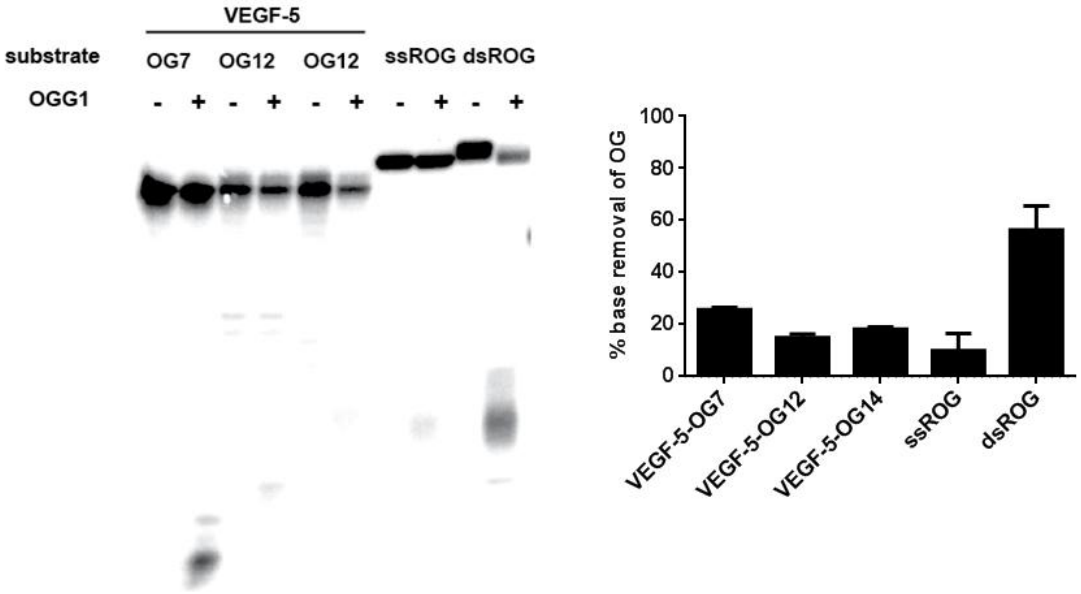

References

1. Luo, W., Muller, J. G., Rachlin, E. M., and Burrows, C. J. (2001) Characterization of hydantoin products from one-electron oxidation of 8-Oxo-7,8-dihydroguanosine in a nucleoside model, *Chem. Res. Toxicol. 14*, 927-938.

2. Fleming, A. M., Alshykhly, O., Zhu, J., Muller, J. G., and Burrows, C. J. (2015) Rates of chemical cleavage of DNA and RNA oligomers containing guanine oxidation products, *Chem. Res. Toxicol.*, DOI: 10.1021/acs.chemrestox.1025b00096.

3. Olsen, C. M., Gmeiner, W. H., and Marky, L. A. (2006) Unfolding of G-quadruplexes: Energetic, and ion and water contributions of G-quartet stacking, *J. Phys. Chem. B 110*, 6962-6969.

4. Zhou, J., Fleming, A. M., Averill, A. M., Burrows, C. J., and Wallace, S. S. (2015) The NEIL glycosylases remove oxidized guanine lesions from telomeric and promoter quadruplex DNA structures, *Nucleic Acids Res. 43*, 4039-4054.

5. Bandaru, V., Blaisdell, J. O., and Wallace, S. S. (2006) Oxidative DNA glycosylases: recipes from cloning to characterization, *Methods in enzymology 408*, 15-33.

6. Odell, I. D., Newick, K., Heintz, N. H., Wallace, S. S., and Pederson, D. S. (2010) Non-specific DNA binding interferes with the efficient excision of oxidative lesions from chromatin by the human DNA glycosylase, NEIL1, *DNA repair 9*, 134-143.

7. Liu, M., Bandaru, V., Holmes, A., Averill, A. M., Cannan, W., and Wallace, S. S. (2012) Expression and purification of active mouse and human NEIL3 proteins, *Protein expression and purification 84*, 130-139.

8. Robey-Bond, S. M., Barrantes-Reynolds, R., Bond, J. P., Wallace, S. S., and Bandaru, V. (2008) Clostridium acetobutylicum 8-oxoguanine DNA glycosylase (Ogg) differs from eukaryotic Oggs with respect to opposite base discrimination, *Biochemistry 47*, 7626-7636.

9. Lim, K. W., Jenjaroenpun, P., Low, Z. J., Khong, Z. J., Ng, Y. S., Kuznetsov, V. A., and Phan, A. T. (2015) Duplex stem-loop-containing quadruplex motifs in the human genome: a combined genomic and structural study, *Nucleic Acids Res*, doi: 10.1093/nar/gkv1355.

10. Agrawal, P., Hatzakis, E., Guo, K., Carver, M., and Yang, D. (2013) Solution structure of the major G-quadruplex formed in the human VEGF promoter in K^+: insights into loop interactions of the parallel G-quadruplexes, *Nucleic Acids Res. 41*, 10584-10592.

11. Phan, A. T., Modi, Y. S., and Patel, D. J. (2004) Propeller-type parallel-stranded G-quadruplexes in the human c-myc promoter, *J. Am. Chem. Soc. 126*, 8710-8716.

12. Patel, D. J., Phan, A. T., and Kuryavyi, V. (2007) Human telomere, oncogenic promoter and 5'-UTR G-quadruplexes: diverse higher order DNA and RNA targets for cancer therapeutics, *Nucleic Acids Res. 35*, 7429-7455.

13. Agrawal, P., Lin, C., Mathad, R. I., Carver, M., and Yang, D. (2014) The major G-quadruplex formed in the human BCL-2 proximal promoter adopts a parallel structure with a 13-nt loop in K^+ solution, *J. Am. Chem. Soc. 136*, 1750-1753.

14. Tong, X., Lan, W., Zhang, X., Wu, H., Liu, M., and Cao, C. (2011) Solution structure of all parallel G-quadruplex formed by the oncogene RET promoter sequence, *Nucleic Acids Res. 39*, 6753-6763.

15. Cogoi, S., and Xodo, L. E. (2006) G-quadruplex formation within the promoter of the *KRAS* proto-oncogene and its effect on transcription, *Nucleic Acids Res. 34*, 2536-2549.

16. Ohnmacht, S. A., Micco, M., Petrucci, V., Todd, A. K., Reszka, A. P., Gunaratnam, M., Carvalho, M. A., Zloh, M., and Neidle, S. (2012) Sequences in the HSP90 promoter form G-quadruplex structures with selectivity for disubstituted phenyl bis-oxazole derivatives, *Bioorg. Med. Chem. Lett. 22*, 5930-5935.

17. Chen, Y., Agrawal, P., Brown, R. V., Hatzakis, E., Hurley, L., and Yang, D. (2012) The major G-quadruplex formed in the human platelet-derived growth factor receptor beta promoter adopts a novel broken-strand structure in K^+ solution, *J. Am. Chem. Soc. 134*, 13220-13223.

18. Mitchell, T., Ramos-Montoya, A., Di Antonio, M., Murat, P., Ohnmacht, S., Micco, M., Jurmeister, S., Fryer, L., Balasubramanian, S., Neidle, S., and Neal, D. E. (2013) Downregulation of androgen receptor transcription by promoter g-quadruplex stabilization as a potential alternative treatment for castrate-resistant prostate cancer, *Biochemistry 52*, 1429-1436.

19. Brown, R. V., Gaerig, V. C., Simmons, T., and Brooks, T. A. (2013) Helping Eve overcome ADAM: G-quadruplexes in the ADAM-15 promoter as new molecular targets for breast cancer therapeutics, *Molecules 18*, 15019-15034.

20. Rodriguez, R., Miller, K. M., Forment, J. V., Bradshaw, C. R., Nikan, M., Britton, S., Oelschlaegel, T., Xhemalce, B., Balasubramanian, S., and Jackson, S. P. (2012) Small-molecule-induced DNA damage identifies alternative DNA structures in human genes, *Nat. Chem. Biol. 8*, 301-310.

21. Wei, D., Todd, A. K., Zloh, M., Gunaratnam, M., Parkinson, G. N., and Neidle, S. (2013) Crystal structure of a promoter sequence in the B-raf gene reveals an intertwined dimer quadruplex, *J. Am. Chem. Soc. 135*, 19319-19329.

22. Huang, W., Smaldino, P. J., Zhang, Q., Miller, L. D., Cao, P., Stadelman, K., Wan, M., Giri, B., Lei, M., Nagamine, Y., Vaughn, J. P., Akman, S. A., and Sui, G. (2012) Yin Yang 1 contains G-quadruplex structures in its promoter and 5'-UTR and its expression is modulated by G4 resolvase 1, *Nucleic Acids Res. 40*, 1033-1049.

23. Chaires, J. B., Trent, J. O., Gray, R. D., Dean, W. L., Buscaglia, R., Thomas, S. D., and Miller, D. M. (2014) An improved model for the hTERT promoter quadruplex, *PLoS ONE 9*, e115580.

24. Palumbo, S. L., Memmott, R. M., Uribe, D. J., Krotova-Khan, Y., Hurley, L. H., and Ebbinghaus, S. W. (2008) A novel G-quadruplex-forming GGA repeat region in the c-myb promoter is a critical regulator of promoter activity, *Nucleic Acids Res. 36*, 1755-1769.

25. Yan, J., Zhao, X., Liu, B., Yuan, Y., and Guan, Y. (2015) An intramolecular G-quadruplex structure formed in the human MET promoter region and its biological relevance, *Mol. Carcinog.*, doi: 10.1002/mc.22330.

26. Wang, Q., Han, G., Ye, J., Gao, X., Niu, H., Zhao, J., Chai, Y., Li, N., and Yin, H. (2014) Characterization of the polycystic kidney disease 2 gene promoter, *Genomics 104*, 512-519.

27. Waller, Z. A., Howell, L. A., Macdonald, C. J., O'Connell, M. A., and Searcey, M. (2014) Identification and characterisation of a G-quadruplex forming sequence in the promoter region of nuclear factor (erythroid-derived 2)-like 2 (Nrf2), *Biochem. Biophys. Res. Commun. 447*, 128-132.

28. Grigg, J. C., Shumayrikh, N., and Sen, D. (2014) G-quadruplex structures formed by expanded hexanucleotide repeat RNA and DNA from the neurodegenerative disease-linked C9orf72 gene efficiently sequester and activate heme, *PLoS ONE 9*, e106449.

29. Fleming, A. M., Muller, J. G., Ji, I., and Burrows, C. J. (2011) Characterization of 2'-deoxyguanosine oxidation products observed in the Fenton-like system Cu(II)/H_2O_2/reductant in nucleoside and oligodeoxynucleotide contexts, *Org. Biomol. Chem. 9*, 3338-3348.

30. Luo, W., Muller, J. G., Rachlin, E. M., and Burrows, C. J. (2000) Characterization of spiroiminodihydantoin as a product of one-electron oxidation of 8-oxo-7,8-dihydroguanosine, *Org. Lett. 2*, 613-616.

31. Fleming, A. M., and Burrows, C. J. (2013) G-Quadruplex folds of the human telomere sequence alter the site reactivity and reaction pathway of guanine oxidation compared to duplex DNA, *Chem. Res. Toxicol. 26*, 593-607.

32. Ye, Y., Muller, J. G., Luo, W., Mayne, C. L., Shallop, A. J., Jones, R. A., and Burrows, C. J. (2003) Formation of ^{13}C-, ^{15}N-, and ^{18}O-labeled guanidinohydantoin from guanosine oxidation with singlet oxygen. Implications for structure and mechanism, *J. Am. Chem. Soc. 125*, 13926-13927.